

Supramolecular-Directed Chiral Induction in Biaryl Derivatives

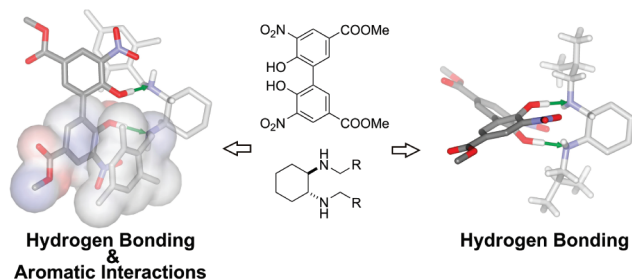
J. Etxebarria,[†] H. Degenbeck,[†] A.-S. Felten,[†] S. Serres,[†] N. Nieto,[†] and A. Vidal-Ferran^{*,†,‡}

[†]Institute of Chemical Research of Catalonia (ICIQ), Av. Països Catalans 16, 43007 Tarragona, Spain, and

[‡]Catalan Institute for Research and Advanced Studies (ICREA), Pg. Lluís Companys 23, 08010 Barcelona, Spain

avidal@icq.es

Received July 17, 2009



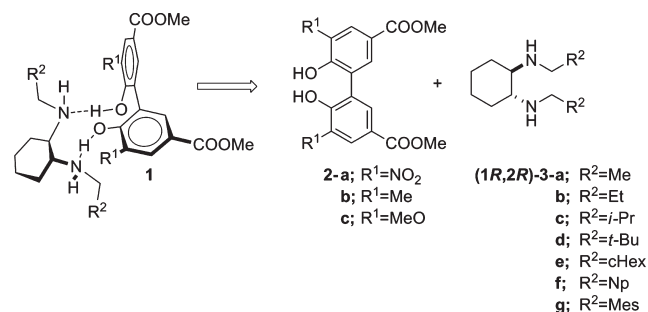
A thermodynamically controlled resolution has allowed for the generation of diastereomerically enriched complexes, by chirality transfer from an enantiopure building block to a dynamically racemic biaryl derivative. A switchable sense of induction could be achieved depending on the substituents of the chiral block.

Hydrogen bonding has long been used as a driving force for chiral recognition and binding, and a great number of chiral supramolecular complexes have been prepared with this strategy.¹ In most cases, chemical and physical properties associated with chirality are due to “static” stereochemistry, the fixed spatial arrangements of atoms. Conversely, dynamic stereochemistry deals with molecular changes and constitutes an interesting alternative strategy for generating

enantio-enriched compounds.² The conformer population of a dynamically racemic mixture (rapidly interconverting enantiomers) can be disturbed from equilibrium by a chiral bias. Some examples of this strategy have been reported,^{1a–c,e,f,h,3} and this paper details our preliminary efforts in the induction and control of axial chirality in stereolabile biaryls, by means of hydrogen bonding. Further, the effects of *orthogonal* binding motifs (aromatic interactions with respect to hydrogen bonding) have proven to be a tool to switch the sense of chiral induction.

We envisaged that supramolecular complexes of the type **1** could be formed from enantiopure diamines **3a–g** and free rotating (*tropos*)^{3a} biphenyl-2,2'-diols **2a–c** by two simultaneous hydrogen bonding interactions between the amino and hydroxyl substituents (Scheme 1). It was reasoned that the multipoint interactions would increase the strength of the complexation process through the chelate effect,⁴ thus preferentially leading to cyclic structures.

SCHEME 1. Design of Hydrogen Bonding-Mediated Complexes 1



Aliphatic amino and phenolic groups can be regarded as complementary hydrogen bonding acceptors and donors, the hydrogen bonding between them has been well studied both experimentally⁵ and theoretically.⁶ The *ortho*-substituents of the phenolic OH groups were essential to our approach: their electronic character, acceptor or donor, should be reflected in an enhanced (or decreased) acidity of the phenol group, and hence in the strength of any resulting hydrogen bond.⁶ For this purpose, compounds **2** with donor ($R^1 = \text{Me}$, **2b**; $R^1 = \text{OMe}$, **2c**) and acceptor groups ($R^1 = \text{NO}_2$, **2a**) were synthesized. Another key strategy was altering the *N*-substituents which, through steric interactions

(1) See for example: (a) Mizutani, T.; Takagi, H.; Hara, O.; Horiguchi, T.; Ogoshi, H. *Tetrahedron Lett.* **1997**, *38*, 1991–1994. (b) Takagi, H.; Mizutani, T.; Horiguchi, T.; Kitagawa, S.; Ogoshi, H. *Org. Biomol. Chem.* **2005**, *3*, 2091–2094. (c) Eelkema, R.; Feringa, B. L. *J. Am. Chem. Soc.* **2005**, *127*, 13480–13481. (d) Breit, B. *Angew. Chem., Int. Ed.* **2005**, *44*, 6816–6825. (e) Morioka, K.; Tamagawa, N.; Maeda, K.; Yashima, E. *Chem. Lett.* **2006**, *35*, 110–111. (f) Ishii, Y.; Onda, Y.; Kubo, Y. *Tetrahedron Lett.* **2006**, *47*, 8221–8225. (g) Ikeda, T.; Hirata, O.; Takeuchi, M.; Shinkai, S. *J. Am. Chem. Soc.* **2006**, *128*, 16008–16009. (h) Suzuki, T.; Ohta, K.; Nehira, T.; Higuchi, H.; Ohta, E.; Kawai, H.; Fujiwara, K. *Tetrahedron Lett.* **2008**, *49*, 772–776. (i) Yu, J.; RajanBabu, T. V.; Parquette, J. R. *J. Am. Chem. Soc.* **2008**, *130*, 7845–7847. (j) Hembury, G. A.; Borovkov, V. V.; Inoue, Y. *Chem. Rev.* **2008**, *108*, 1–73. (k) Breuil, P. A. R.; Patureau, F.; Reek, J. N. H. *Angew. Chem., Int. Ed.* **2009**, *48*, 2162–2165 and references cited therein.

(2) Wolf, C. *Dynamic Stereochemistry of Chiral Compounds: Principles and Applications*; The Royal Society of Chemistry: Cambridge, UK, 2008.

(3) See for example: (a) Walsh, P. J.; Lurain, A. E.; Balsells, J. *Chem. Rev.* **2003**, *103*, 3297–3344. (b) Costa, A. M.; Jimeno, C.; Gavenonis, J.; Carroll, P. J.; Walsh, P. J. *J. Am. Chem. Soc.* **2002**, *124*, 6929–6941 and references cited therein.

(4) (a) Blackman, A. G. *C. R. Chim.* **2005**, *8*, 107–119. (b) Bowman, D. C. *J. Chem. Educ.* **2006**, *83*, 1158–1160.

(5) (a) Gurka, D.; Taft, R. W.; Joris, L.; Schleyer, P. v. R. *J. Am. Chem. Soc.* **1967**, *89*, 5957–5958. (b) Kraemer, R.; Zundel, G. *J. Chem. Soc., Faraday Trans.* **1990**, *86*, 301–305. (c) Koll, A.; Rospenk, M.; Sobczyk, L. *J. Chem. Soc., Faraday Trans. 1* **1981**, *77*, 2309–2314. (d) Albrecht, G.; Zundel, G. *J. Chem. Soc., Faraday Trans. 1* **1984**, *80*, 553–561. (e) Pawelka, Z.; Kuc, T. *Pol. J. Chem.* **2001**, *75*, 845–855.

(6) (a) Gilli, P.; Pretto, L.; Bertolasi, V.; Gilli, G. *Acc. Chem. Res.* **2009**, *42*, 33–44. (b) Szatylowicz, H. *J. Phys. Org. Chem.* **2008**, *21*, 897–914. (c) Hunter, C. A. *Angew. Chem., Int. Ed.* **2004**, *43*, 5310–5324. (d) Fedorowicz, A.; Koll, A.; Mavri, J. *Theor. Chem. Acc.* **2003**, *109*, 220–228.

TABLE 1. UV and CD Spectral Data of Hydrogen-Bonded Complexes

entry	complex	solvent	UV data: λ_{\max} , $^a \epsilon$ b	K^c	CD Data: λ_{\max} , $^a \Delta \epsilon$ b
1	2a + (1 <i>R</i> ,2 <i>R</i>)- 3c	THF	386, 7.4×10^3	8.1×10^5	— ^e
2	2b + (1 <i>R</i> ,2 <i>R</i>)- 3c	THF	280, 2.2×10^4	1.3×10^3	— ^e
3	2c + (1 <i>R</i> ,2 <i>R</i>)- 3c	THF	278, 2.9×10^4	2.2×10^2	— ^e
4	2a + (1 <i>R</i> ,2 <i>R</i>)- 3a	toluene	385, 6.9×10^3	2.0×10^5	389, 0.07
5	2a + (1 <i>R</i> ,2 <i>R</i>)- 3b	toluene	386, 6.7×10^3	2.7×10^5	395, 0.25
6	2a + (1 <i>R</i> ,2 <i>R</i>)- 3c	toluene	383, 6.4×10^3	2.0×10^5	381, 0.51
7	2a + (1 <i>R</i> ,2 <i>R</i>)- 3d	toluene	382, 6.9×10^3	5.6×10^4	384, 0.98
8	2a + (1 <i>R</i> ,2 <i>R</i>)- 3e	toluene	384, 6.6×10^3	2.7×10^5	394, 0.34
9	2a + (1 <i>R</i> ,2 <i>R</i>)- 3f	toluene	385, 6.0×10^3	3.9×10^5	395, 0.37
10	2a + (1 <i>R</i> ,2 <i>R</i>)- 3g	toluene	379, 8.5×10^3	2.5×10^4	344, -1.55

^aIn nm. ^bIn $M^{-1} \cdot cm^{-1}$. ^cIn M^{-1} , mean value of at least two measurements. ^dUV data for **2**: **2a** (352, 7.3×10^3 in THF; 358, 7.1×10^3 in toluene); **2b** (274, 9.8×10^3 in THF); **2c** (273, 2.1×10^4 in THF). ^eNot measured.

with the biaryl derivatives, would be responsible for the chiral induction. A wide range of diamines with sterically different *N*-substituents were synthesized, **3a–g**, in order to study their influence on the complexation and chiral induction processes. An ester group was incorporated in the biphenyl-2,2'-diol subunit, allowing for the simple transformation into a wide variety of binding groups for future catalytic applications.

Compounds **2a–c** and amines **3a–g** were synthesized in good yields by well-established synthetic transformations.⁷

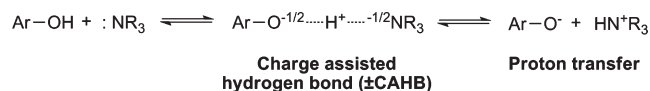
Complexation studies between biaryl derivatives **2** and chiral diamines **3** were made by means of UV–vis spectroscopy. Titration of a solution of **2** with **3** led to a decrease in intensity of the initial biaryl band and the appearance of a new red-shifted band (see Table 1). Equilibrium constants were extracted by analyzing the UV–vis titration data⁷ and are summarized in Table 1.

The formation of complexes derived from **2a** could be confirmed by NMR, clearly showing an interaction between the biaryl and amine in a 1:1 ratio. In all cases, NMR signals for the complexes were in agreement with a C_2 -symmetric averaged structure. Variable-temperature ¹H NMR analysis (298–200 K, toluene-*d*₆) showed only one set of signals across the whole range of studied temperatures, indicating that either one main diastereoisomer was present or that the exchange processes were faster (even at 200 K) than the NMR time scale.

The binding constant *K* was found to decrease 3 orders of magnitude between **2a** and **2c** (cf. entries 1–3, Table 1). Literature precedents suggest that a doubly charged-assisted H-bond (\pm CAHB;^{6a} Scheme 2; i.e. hydrogen bonds derived from an acid–base equilibrium, such as between the nitro derivative **2a** and amines **3**)^{5,6,8} would be stronger than an ordinary hydrogen bond, such as in **2b**, **2c**, and **3**. *pK*_a values of the *o*-nitrophenol unit and the protonated amine are relatively close⁹ and a \pm CAHB should be facilitated. \pm CAHB can lead to a complete proton transfer. However, UV–vis studies on our system suggest that proton transfer is

not a major process.¹⁰ The UV–vis spectrum of sodium 5,5'-bis(methoxycarbonyl)-3,3'-dinitrobiphenyl-2,2'-bis(olate) (Na₂-**2a**) in a THF solution¹¹ shows an intense band with a maximum centered at 441 nm.⁷ Under identical conditions, a mixture of **2a** and **3c** showed an absorption band with a maximum centered at 386 nm. Assuming that the intensity of the absorption at 441 nm arises exclusively from the phenolate chromophore from the complexation process between **2a** and **3c**, then the extent of the proton transfer can be estimated to 8% as a maximum. Regarding the sterics of the complexation process, *K* values for **2a** and **3a–g** are similar (cf. entries 4–10, Table 1), indicating that the size of the substituents of the amino groups has a small effect on the strength of the complexation process.

SCHEME 2. Charged Assisted H-Bond and Proton Transfer



The complexation of **2a** and **3c** was investigated by isothermal calorimetry (ITC). Very good agreement between the *K* values obtained by UV and ITC (*K* = $2 \times 10^5 M^{-1}$ in toluene and *K* = $5 \times 10^5 M^{-1}$ in THF, both at 298 K; see entries 1 and 6 in Table 1 for *K* values obtained by UV) was observed. A 1:1 ratio between **2a** and **3c** was deduced from ITC data.⁷ ΔH and ΔS values (−14.2 kcal/mol, −23.3 cal/mol/K, 298 K in toluene) were also extracted from the titration data. ΔH is in agreement with a \pm CAHB between acidic phenols and amines (ΔH = −9.8 kcal/mol for *p*-nitrophenol and dibutylamine^{8d}). An overall decrease for ΔS in the complexation process was expected as a consequence of the entropically unfavorable chelate formation process.

Each conformer of **2** could react with the enantiopure amine **3** forming two different diastereomeric complexes **1** (see Scheme 3), via a thermodynamically controlled resolution. The stereochemical outcome of such an asymmetric process would depend on the relative thermodynamic stabilities of (*R,R,M*)-**1** and (*R,R,P*)-**1**.

CD spectra of complexes **1** showed a Cotton effect in all cases (see Table 1), indicating that the biphenyl unit is twisted with a predominant screw sense. The diastereoisomer

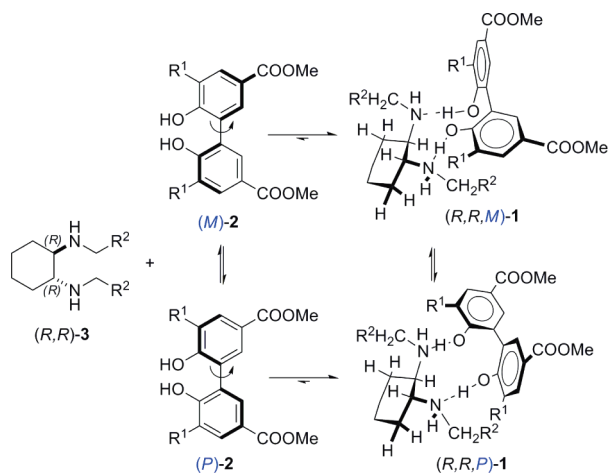
(7) See the Supporting Information for details.

(8) (a) Mizutani, T.; Takagi, H.; Ueno, Y.; Horiguchi, T.; Yamamura, K.; Ogoshi, H. *J. Phys. Org. Chem.* **1998**, *11*, 737–742. (b) Hudson, R. A.; Scott, R. M.; Vinogradov, S. N. *Spectrochim. Acta, Part A* **1970**, *26*, 337–343. (c) Baba, H.; Matsuyama, A.; Kokubun, H. *Spectrochim. Acta, Part A* **1969**, *25*, 1709–1722. (d) Libus, W.; Mecik, M.; Sulek, W. *J. Solution Chem.* **1977**, *6*, 865–879. (e) Dwivedi, P. C.; Banga, A. K.; Sharma, N. *Spectrochim. Acta, Part A* **1986**, *42A*, 623–629. (f) Pillay, M. K.; Umamaheswari, A. *J. Indian Chem. Soc.* **1991**, *68*, 62–64.

(9) *pK*_a of 7.2 (Wang, S.-P.; Chen, H.-J. *J. Chromatogr., A* **2002**, *979*, 439–446) and 10.7 (Fu, S. *Analyst* **1998**, *123*, 1487–1492) have been reported for 2-nitrophenol and dimethylammonium. $\Delta pK_a = pK_a(Ar-OH) - pK_a(HN^+R_3)$ can be estimated as 3 for our system.

(10) This result is in agreement with reported data in the literature, as the extent of proton transfer in CCl₄ for several chloro-substituted phenol–amine systems with $\Delta pK_a \approx 3$ has been reported to be roughly less than 15%; see: Albrecht, G.; Zundel, G. *J. Chem. Soc., Faraday Trans. 1* **1984**, *80*, 553–561.

(11) Na₂-**2a** was generated by treatment of a solution of **2a** in THF with a slight excess of NaH. THF was used instead of toluene for solubility reasons.

SCHEME 3. Diastereoselective Complexation between **2** and **3**

populations are biased during the complexation process, and the observed CD signal is a factor of the degree of twist and the relative populations of the complexes (which would cancel each other out if equimolarly present). Complexes derived from (R,R) -**3a–f** showed a positive Cotton effect and the highest CD amplitude was observed for the amine **3d** (see Figure 1): the bulky *N*-neopentyl substituents on **3d** preferentially twist the biaryl unit to a greater extent. This observation should only be considered as an estimate, since it has been reported that major alterations in the chromophore, i.e. dihedral angle in the biaryl unit, lead to changes in the position and intensity of the CD bands in related chromophores.¹² Strikingly, the sense of helical screw of the biaryl unit is reversed in the complex containing *N*-mesitylmethyl amine **3g** (entry 10, Table 1). These results indicate that the dynamically racemic biaryl derivative **2a** can be readily fixed upon complexation with either a *P*- or *M*-torsion depending on the nature of the *N*-substituents.

To gain a deeper insight into the three-dimensional structure of these complexes, full level DFT geometry optimization of all the C_2 -symmetric diastereoisomers **2a** + (R,R) -**3c** (positive Cotton effect) and **2a** + (R,R) -**3g** (negative Cotton effect) was carried out. Due to its good performance with weak noncovalent interactions, MPWB1K¹³ density functional theory was used.⁷ Computed relative energies are summarized in Table 2.

TABLE 2. Computed Relative Energies for **2a** + **3c** and **2a** + **3g**

diastereoisomer 2a + $(1R,2R)$ - 3c			diastereoisomer 2a + $(1R,2R)$ - 3g		
entry	diastereoisomer	energy ^a	entry	diastereoisomer	energy ^a
1	R_C, R_C, S_N, S_N, P^b	0.0	5	R_C, R_C, R_N, R_N, M	0.0
2	R_C, R_C, R_N, R_N, P	0.2	6	R_C, R_C, S_N, S_N, P	3.6
3	R_C, R_C, S_N, S_N, M	2.4	7	R_C, R_C, R_N, R_N, P	5.0
4	R_C, R_C, R_N, R_N, M	3.2	8	R_C, R_C, S_N, S_N, M	10.4

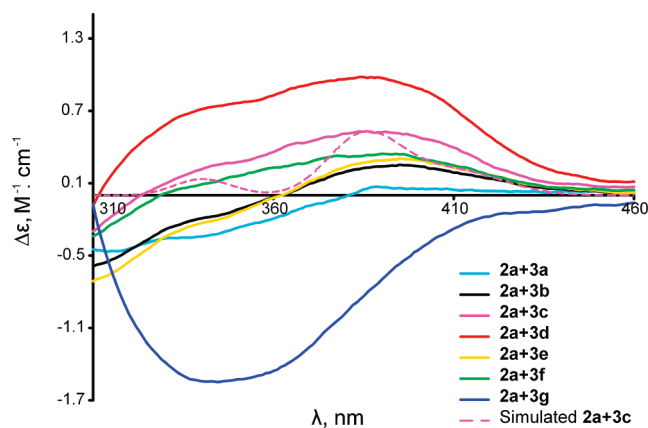
^aIn kcal/mol. ^bThe first two characters refer to configuration of the *N*-substituted carbons in the amine unit **3**, the following two indicate the configurations for the tetrahedral nitrogen atoms upon complexation [*R* or *S*; substituent priorities: C(ring) > C(*N*-substituent) > H(O) > H(N)] and the last one indicates the sense of screw of the chiral axis in the biaryl unit.

(12) Di Bari, L.; Pescitelli, G.; Salvadori, P. *J. Am. Chem. Soc.* **1999**, *121*, 7998–8004.

(13) (a) Zhao, Y.; Schultz, N. E.; Truhlar, D. G. *J. Chem. Theory Comput.* **2006**, *2*, 364–382. (b) Zhao, Y.; Truhlar, D. G. *J. Chem. Theory Comput.* **2007**, *3*, 289–300.

These studies indicated that the most stable diastereoisomer for the isobutyl-substituted complex has a *P* configuration (entry 1, Table 2), while calculations on the mesityl-substituted complex (**2a** + **3g**) indicate an *M* configuration of the chiral biaryl unit (entry 5, Table 2). Each of the two mesityl substituents is arranged in off-face stacking with the nitro-substituted aryl rings, thus facilitating simultaneous π (CH) interactions between the aromatic rings.¹⁴ Finally, calculations predict a slightly higher energy gap between diastereoisomers differing in the configuration at the biaryl unit (2.4 kcal/mol for the isobutyl and 3.6 kcal/mol for the mesityl complexes), which may account for the higher magnitude of the Cotton effect in the mesityl-substituted complex.

The geometry optimized coordinates from the most stable **2a** + **3c** diastereoisomer (R_C, R_C, S_N, S_N, P ; entry 1, Table 2) were used in a time-dependent density functional theory (TDDFT) prediction of circular dichroism data, using B3LYP and aug-cc-pVDZ,⁷ since this methodology has proven to be reliable in CD predictions.¹⁶ Agreement between experimental and computed CD data is good (Figure 1)¹⁷ and the *P*-helical screw sense of the biaryl unit in the isobutyl-substituted complex was confirmed by comparison of the experimental sign of the Cotton effect with its calculated value.

FIGURE 1. CD data for complexes **1**.¹⁵

In conclusion, a thermodynamically controlled resolution has allowed the generation of diastereomerically enriched supramolecular complexes, by chirality-transfer from an enantiopure building block to a dynamically racemic biaryl derivative. The formation of two doubly charged-assisted H-bonds can be regarded as the driving force for the generation of highly stable complexes ($K > 10^5 \text{ M}^{-1}$). This work shows the potential of noncovalent interactions [hydrogen bond and π (CH)] for transmission and control of chirality at the molecular level: a chirally oriented conformation can be created not only by stereogenic elements of a chiral inducer, but also by additional supramolecular interactions which are capable of reversing the sense of induction. Work is in

(14) Hunter, C. A.; Lawson, K. R.; Perkins, J.; Urch, C. J. *J. Chem. Soc., Perkin Trans. 2* **2001**, 651–669.

(15) Amines **3a–g** were CD-silent in the 310–460 nm range.

(16) Stephens, P. J.; McCann, D. M.; Butkus, E.; Stoncicus, S.; Cheeseman, J. R.; Frisch, M. J. *J. Org. Chem.* **2004**, *69*, 1948–1958.

(17) The computed amplitude of the CD data was normalized to the experimental values.

progress to exploit this strategy in the preparation of sensors and chiral ligands for asymmetric transformations of interest.

Experimental Section

Preparation of Hydrogen Bonded Complexes 1. Compounds **2** (0.024 mmol) and **3** (0.024 mmol) were mixed and dried under vacuum for 12 h. The required solvent (dry and degassed CDCl₃ (1.00 mL) was used for NMR analysis of the hydrogen bonded complexes) was then added. See the Supporting Information for the spectroscopical data of **2a** + (1*R*,2*R*)-**3a–g**. As a representative example, **2a** + (1*R*,2*R*)-**3e**: ¹H NMR (400 MHz, CDCl₃) δ 0.89 (m, 5H), 1.15 (m, 10H), 1.42 (m, 2H), 1.66 (m, 12H), 2.13 (m, 2H), 2.39 (m, 3H), 2.77 (dd, *J* = 11.7, 6.5 Hz, 2H), 3.94 (s, 6H), 8.23 (d, *J* = 2.4 Hz, 2H), 8.57 (d, *J* = 2.4 Hz, 2H); ¹³C NMR (100 MHz, CDCl₃) δ 24.3 (CH₂), 25.5 (CH₂), 26.1 (CH₂), 29.1 (CH₂), 30.8 (CH₂), 36.7 (CH), 52.0 (CH₃), 52.1 (CH₂),

60.5 (CH), 117.9 (C), 127.1 (CH), 132.3 (C), 136.3 (CH), 140.1 (C), 160.0 (C), 165.8 (C); MS (TOF MS ES+) calcd for [C₃₆H₅₀N₄O₁₀H]⁺ required 699.36, found 699.4; calcd for [C₃₆H₅₀N₄O₁₀Na]⁺ required 721.34, found 721.3.

Acknowledgment. We thank MICINN (Grant CTQ2008-00950/BQU), DURSI (Grant 2009GR623), Consolider Ingenio 2010 (Grant CSD2006-0003), and ICIQ Foundation for financial support. Prof. Feliu Maseras (ICIQ) is gratefully acknowledged for advice in the computational studies.

Supporting Information Available: Experimental details, characterization data, and NMR spectra for compounds **1**, **2**, and **3**, general procedures used for UV–vis, CD and computational data, and molecular modeling coordinates. This material is available free of charge via the Internet at <http://pubs.acs.org>.